كلية الهندسة بشبرا
FACULTY OF ENGINEERING AT SHOUBRA
ERJ
ISSN:1687-1340

ENGINEERING RESEARCH JOURNAL (ERJ)
Volume (52) , Issue (1)
January 2023, pp:94-100
https://erjsh.journals.ekb.eg

Standalone PV-Based Water Pumping System Optimization using Jellyfish Technique

Mohamed Selmy[1], Mohsen Z. El sherif[1], Miral Salah Noah*[2], and Islam M. Abdelqawee[1]
[1] Department of Electrical Power Engineering , Faculty of Engineering at Shoubra, Benha University, Cairo, Egypt .
[2] Department of Electrical Power Engineering, Faculty of Engineering, Cairo University, Cairo, Egypt
***** Corresponding author.
E-mail:miral.nooh@gmail.com,Mohamed.selmy@feng.bu.edu.eg,islam.ahmed@feng.bu.edu.eg,elsherif.mohsen@yahoo.com.

Abstract: Because of the increasing and escalating demand on energy sources, utilizing renewable energy sources efficiently becomes mandatory. This paper aims to construct and discuss efficient and low-cost configuration of standalone PV water pumping system with three-phase induction motor. This configuration is achieved by using optimized PI-controllers with the Jellyfish optimizer and a high gain DC to DC converter with maximum power point tracking technique to extract maximum power from the PV system. In addition to the high gain DC to DC converter, the proposed system consists of PV array, DC to DC bidirectional converter with batteries in order to save excess PV power and reuse it when there is no enough output power for the system, three-phase inverter, three-phase induction motor, and pump to drive the water. The proposed system succeeded to keep the total harmonic distortion for the AC output voltage within 0.61%, and keep DC bus voltage ripple factor within 0.2%, both are within acceptable limits. The system is designed, modeled, and simulated in detail using MATLAB/Simulink software to evaluate the performance under fast variations of climatic profile.

Keywords: PV standalone system, water pumping, Jellyfish optimization.

1. INTRODUCTION

Due to the increased population and global warming, the conventional energy sources are decreasing rapidly, and people are shifting toward the usage of renewable energy sources [1]. Some remote areas are deprived of electricity network, thus development of photovoltaic (PV) renewable energy systems opened such ways for solving this problem, these areas have been isolated due to the unavailability of the local grid nearby and extension will be very expensive [1] [2].

PV system is affected by three main factors; irradiation, load type, and atmospheric temperature. So maximum power point tracking techniques are used to extract maximum power from PV when atmospheric conditions are changed [2].

PV water pumping applications can use different types of motors based on efficiency, availability, reliability, and cost. AC induction motors are widely used because of reliability and cheapness [3]. DC/AC converters are used to transfer power from dc source to ac source. Space vector pulse width modulation is used with the 3-ph inverter to control output AC voltage across 3-ph motor terminals.

In PV pumping applications, induction motors have good performance compared to other motors as it's very robust, cheap, high efficient, and needs low maintenance [4] [5].

Different PV water pumping system configurations are discussed, in [6], MPPT based on incremental conductance technique was used to get maximum power from PV system and scalar control on induction motor.

In [7], off-grid photovoltaic pumping application has been driven by brushless DC motor. Different algorithms are used to get maximum power such as Perturb and observe and fuzzy logic control algorithms. Brushless DC motor is efficient, but rotor position is known by using hall sensors which increases system cost and complexity [8].

In [9], genetic algorithms (GA) optimization tool was applied on perturb and observe and fuzzy techniques MPPT algorithms, permanent magnet DC motor is used to drive the pump. This motor is not very popular as it rare and expensive [10].

Genetic algorithm is used to optimize different algorithms based on basics of biological evolution [11]. Although, this technique doesn't ensure identification of global minimum, and it is not very effective with complex or large problems, as it requires much time to fine tune parameters [12].

In this paper, PV system is used to supply power to 3-ph induction motor to drive water pump. Bidirectional converter and batteries are used to supply power when power from PV system is low and not enough for the motor. 3-ph inverter is used to convert DC volt to AC volt suitable with the motor type. PI controllers are used to control system converters and inverters, Jelly Fish optimization technique is used to optimize controllers gains, also jelly fish optimization tool is used to select parameters of the high gain DC-DC converter to maintain current ripples and voltage ripples within tolerable limits.

Main contributions of this paper are:

- Analysis, and design of the dc-dc high gain converter used in water pumping application.
- System performance enhancement using optimized PI controllers by JF optimizer.
- The proposed system can keep total harmonic distortion for the AC output voltage, and DC bus voltage ripple factor within acceptable limits.

The paper is organized as follows; system description is presented in section II, while system modeling is developed in section III. Section IV shows the system design in details and simulation results as well as discussion are given in section V. Finally, section VI presents conclusion.

2.SYSTEM DESCRIPTION

PV pumping system consists of PV modules, high gain DC-DC converter, MPPT algorithms to control PV modules, and battery with bidirectional converter to supply power to induction motor (IM) when PV power isn't enough. Bidirectional DC–DC converter transfers power between two DC sources in both directions, three-phase inverter, and a centrifugal pump driven by IM as shown in figure 1.

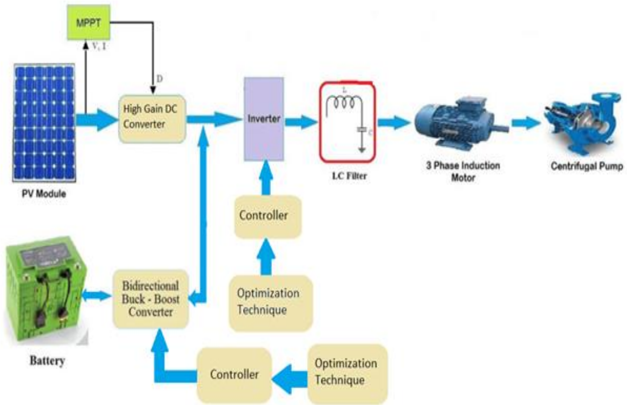

Fig 1. Schematic diagram of the pumping system

3.SYSTEM MODELING

a. PV Module

From the equivalent circuit given in figure 2, the output current can be calculated as follows [13,14,15]:

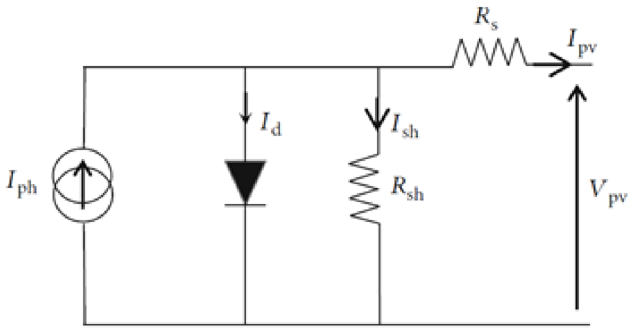

Fig 2. PV Module equivalent circuit

$$I_{pv} = I_{ph} - I_o(\exp\frac{q(V_{pv}+R_s I_{PV})}{\alpha KTN_s} - 1) - \frac{(V_{pv}+I_{PV}R_s)}{R_{sh}} \quad (1)$$

$$I_{ph} = (I_{sc} + K_i(T - 298.15))\frac{G}{1000} \quad (2)$$

$$I_o = \frac{I_{sc} + K_i(T - 298.15)}{\exp((q(V_{oc}+K_v)(T-298.15))/(\alpha KTN_s)) - 1} \quad (3)$$

Where I_{pv} is PV output current, I_{ph} is the photo current, I_o is the reverse saturation current, q is the electron charge, T is the cell temperature, G is the sun insulation, R_s is the series resistance, R_{sh} is the shunt resistance, and α is the diode ideality factor.

a. High Gain DC-DC Converter:

High gain step up DC-DC converter can give two different high voltage levels as shown in figure 3. High voltage loads are connected to the capacitor C_2. Loads that need less voltage are connected to capacitor C_1. Controlled switches open and close periodically depend on given duty cycle to control voltage values. Switches need only one control signal, thus control complexity is reduced.

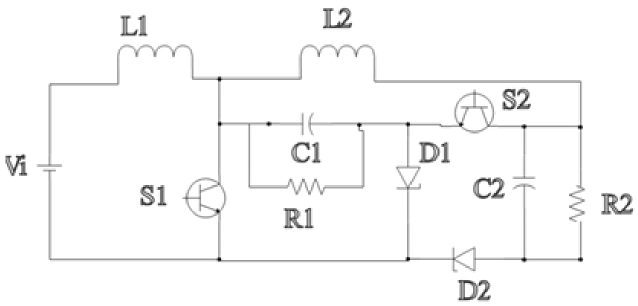

Fig 3. Schematic diagram of high gain Boost converter

There are two modes of operation for this converter which are discussed as follows.

Case I: Switches S1, S2 are Turned off:

In this case, controlled switches are OFF, which forward biases the diodes D_1, D_2, as shown in figure. 4. Then, input V_i and inductors (L_1 and L_2) energize the capacitors (C_1 and C_2) and supply power to the loads.

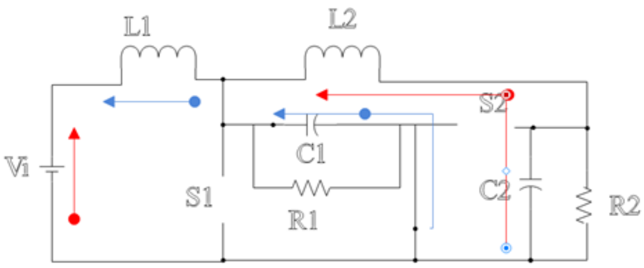

Fig 4. The equivalent circuit of high gain boost converter when switches are OFF

Apply KVL on the right circuit, then:

$$V_i = V_{C1} + V_{L1} \quad (4)$$

$$L_1 \frac{di_{L1}}{dt} = V_i - V_{C1} \quad (5)$$

Apply KVL on the left circuit, then:

$$V_{L2} = V_{C1} - V_{C2} \quad (6)$$

$$L_2 \frac{di_{L2}}{dt} = V_{C1} - V_o \quad (7)$$

Thus, L_2 is written as follows:

$$L_2 = \frac{|(V_{C1} - V_O)|(1-D)T}{\Delta I_{L2}} \quad (8)$$

Apply KCL, the currents passing through inductors L_1 and L_2 are found to be as follows:

$$I_{L1} = I_{L2} + I_{C1} \quad (9)$$

$$C_1 \frac{dV_{C1}}{dt} = I_{L1} - I_{L2} \quad (10)$$

$$I_{L2} = I_{C2} + \frac{V_o}{R} \quad (11)$$

$$C_2 \frac{dV_{C2}}{dt} = I_{L2} - \frac{V_o}{R} \quad (12)$$

Where,

V_i is Low voltage source, V_{L1} is Voltage across inductor L_1, V_{L2} is Voltage across inductor L_2, V_{C1} is Voltage across capacitor C_1, V_{C2} is Voltage across capacitor C_2, T_s is the switching time of controlled switches, D is duty cycle of controlled switches.

Case II: Switches S1, S2 are Turned On:

In this case, the controlled switches are ON, which reverse biases the diodes D_1, D_2 as shown in Figure 5. Then, both the capacitors (C_1 and C_2) energize the inductors (L_1 and L_2).

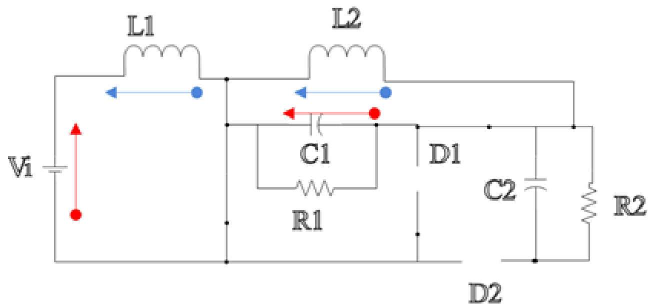

Fig 5. The equivalent circuit of high gain boost converter when switches are ON

Apply KVL on the right circuit, then:

$$V_{L1} = V_i \quad (13)$$

$$V_i = L_1 \frac{di_{L1}}{dt} \quad (14)$$

Thus, L_1 will be as follows:

$$L_1 = \frac{V_i DT}{\Delta i_{L1}} \quad (15)$$

Apply KVL on the left circuit, then:

$$V_{L2} = V_{C1} \quad (16)$$

Average voltage across inductor L_1 equals zero:

$$V_i DTs + (V_i - V_{C1})(1-D)T_s = 0 \quad (15)$$

Then voltage across C_1 will be as follows:

$$V_{C1} = \frac{V_i}{1-D} \quad (16)$$

Average voltage across inductor L_2 equals zero:

$$V_{C1} DT_s + (V_{C1} - V_{C2})(1-D)T_s = 0 \quad (17)$$

$$\frac{V_{C1}}{V_{C2}} = 1 - D \quad (18)$$

Substitute eqn. (18) in eqn. (20), then voltage across C_2 will be as follows:

$$V_{C2} = \frac{V_i}{(1-D)^2} \quad (19)$$

Apply KCL, current passing through capacitor C_2 is same current passing through load as follows:

$$i_{C2} = \frac{V_o}{R} \quad (20)$$

$$C_2 \frac{dV_{C2}}{dt} = \frac{V_o}{R} \quad (21)$$

$$C_2 = \frac{V_o DT}{R \Delta V_{C2}} \quad (22)$$

Now it's shown from equation (21), the voltage gain at capacitor C_2, is significantly high compared to the conventional Boost converter.

a. Centrifugal Pump

Water pump is an electromechanical machine that is utilized to increase water pressure to move it from one point to another, centrifugal pump load torque T_r is given as follows:

$$T_r = Kn^2 \qquad (23)$$

Where K is constant, and n is the pump speed (rpm)

.

4.Control Strategies and Optimization

a. Control Strategies

Perturb and observe (P&O) MPPT algorithm, given in figure 6, is applied to extract maximum power from PV system. P&O controls the duty cycle of the high gain DC-DC converter, where the PV voltage and current are measured to measure output power. when voltage increase, power increases then duty cycle increases in same direction, otherwise duty cycle is reversed [16].

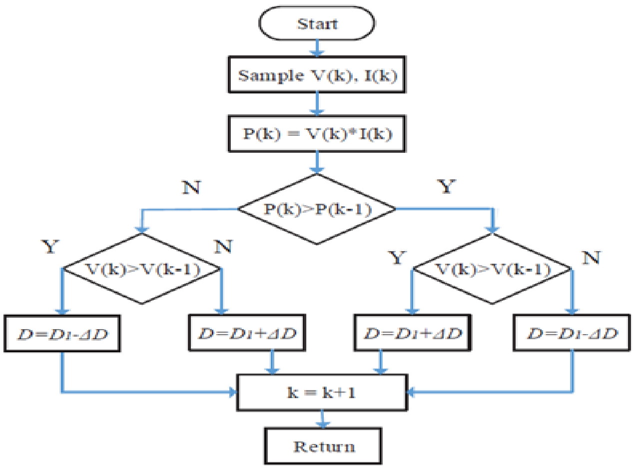

Fig 6. P&O flow chart

PI (proportional integral) controllers are used in industrial control applications to regulate process variables. In this paper different PI controllers are used. First PI controller is used in the bidirectional converter to maintain DC bus voltage at certain required value. Second PI controller as well as SVPWM are used with the three-phase inverter to control the output AC voltage delivered to the three-phase motor terminals.

b. Optimization

PI-controller gains need to be optimized to minimize system error and make it more stable and reliable. Therefore, Jellyfish (JF) optimization technique is applied on PI-controller gains to find their optimum values. JF optimization technique is a metaheuristic algorithm that is taken from behavior of JF in oceans. Simulation of search behavior of JF includes following the ocean current, motions inside a JF swarm (passive and active motions), time control mechanism for switching between movements, and their convergences into JF bloom [17]. The process of JF food search is ordered as following:

- JF movements through swarm.
- chasing ocean current to initiate JF bloom.
- JF movements in ocean are shown in figure 7.

The JF algorithm considers following principles:

- Time control procedure manages switching between two JF advanced movements.
- JF moves towards areas where attainable amount of food is shown.
- The measure of founded food is controlled by location and its related target function.

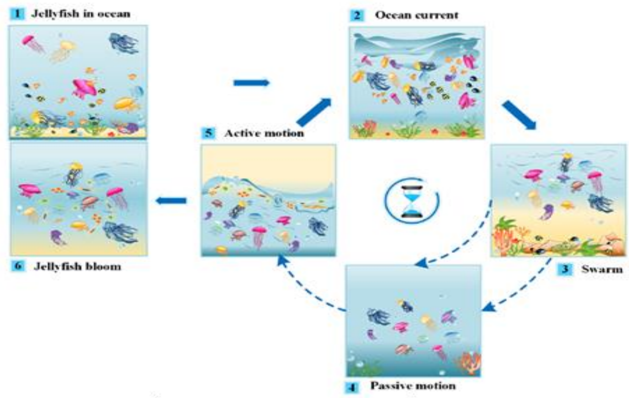

Fig 7. JF movements in ocean

In this proposed system, JF is applied in this system to select PI controllers gains with the following parameters values.

Number of populations = 40,

Maximum number of iterations = 5,

Objective function is to select PI gains which can minimize error signal

$$\text{Integral absolute error} = \int |e|\, dt \qquad (26)$$

For the first PI controller, error signal (e) is the difference between DC bus reference and actual voltages.

For the second PI, error signal is the difference between reference and actual AC output voltages.

5.SYSTEM DESIGN

A case study for a group of houses located in AL-Kharijah Oasis, Egypt, consists of 5 houses, each consists of 4 members, average water consumption is 20 m^3/day which is 0.83 m^3/hr, so for the group total consumption is 4.1 m^3/hr. The pump parameters are selected as illustrated in TABLE. 1. Induction motor is selected to be suitable with the pump to drive water. Average solar irradiation in Al-Kharijah oasis is around 6.6 kWh/m^2. Water head height equals 65 meters.

TABLE. 1 Pump characteristics

Rated power (hp)	5
Maximum head (m)	95
Pump body	Stainless steel

$$P_{pv} = \frac{g.\rho_s.Q_s.T_h}{3600.G.\eta_p.(1-\rho_l)} \quad (24)$$

Where, P_{pv} is the PV power, g is earth gravity acceleration, ρ_s is water density, Q_s is water needed per day (m^3/day), T_h is Total head (meter), η_p is pump efficiency, and ρ_l is system losses [18]. Substitute in Eqn. (26) then, $P_{pv} = 5.7$ kW

The selected PV array is 5 parallel strings, and 6 series modules per string.

PV module data and DC-DC converter circuit parameters are calculated using equations (8, 15, and 24), and the motor parameters are selected from [19] as shown in TABLE. 2.

TABLE. 2 System Parameters [19]

PV module power (Watt)	195.4
V_{oc} open circuit voltage (Volt)	45
I_{sc} short circuit current (Amp)	5.56
Voltage at maximum power (Volt)	37.5
Current at maximum power (Amp)	5.21
Number of cells per module	72
Battery type	Lithium-ion
Battery nominal voltage (Volt)	300
Initial state of charge (%)	75
Rated battery capacity (AH)	600
High gain converter inductor L_1 (H)	0.322
High gain converter inductor L_2 (H)	0.46
High gain converter capacitor C_1 (F)	0.0014
High gain converter capacitor C_2 (F)	0.0014
Induction motor type	Squirrel-cage
Motor rated power (hp)	5.5
Motor nominal voltage (Volt)	400
Motor rated speed (rpm)	1430
Model	NKV 10T

6. Simulation Results and Discussion

a. The proposed system is designed and simulated using MATLAB Simulink. Table 3 describes PI controllers gains when JF optimization applied, and when gains selected by fine tuning.

Table. 3 PI gains

	JF optimization	Fine Tuning
Kp1	0.001	0.05
KI1	0.5	0.2
Kp2	4	1.1
Ki2	1.3	1.5
Kp3	22.3	25
Ki3	30.2	15

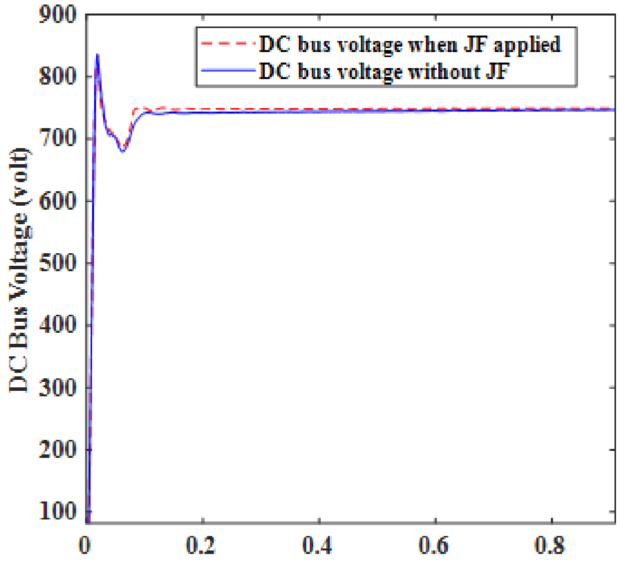

Fig. 8 DC bus voltage level comparison

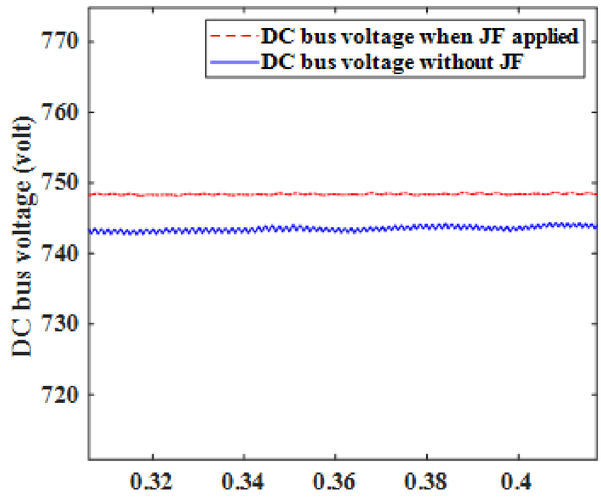

Fig.9 Detailed DC bus voltage

Figure 8, and figure 9 show the difference between dc bus voltage level when JF optimization is applied to the system.

It's clear from figures that when JF is applied the dc voltage is much better.

From previous figures (8,9) voltage ripple can be calculated:

- DC voltage ripples when JF is applied equals 0.2%.
- DC voltage ripples without JF applied equals 0.9%.

AC output voltage across induction motor terminals in both cases is shown in figure.10.

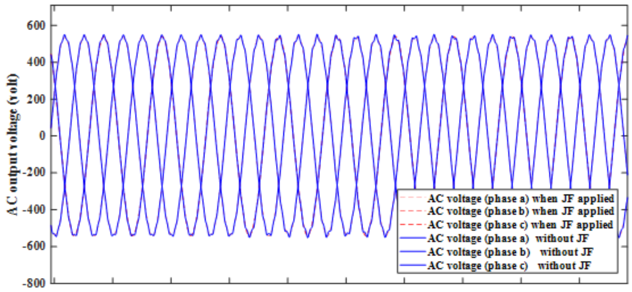

Fig11. AC output voltage

Figure .11 compares between AC output voltage in both cases, it's clear that when the JF optimization is applied the output ac wave is improved, and total harmonic distortion is calculated for the AC wave when the JF is applied to the system using Fast Fourier Transform on Matlab Simulink as shown in figure 12. THD as shown is 0.61%.

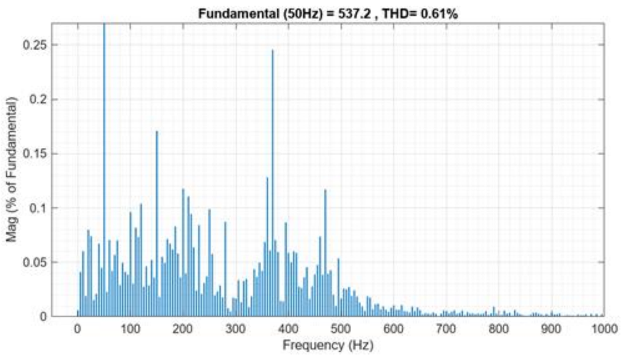

Fig 12. Total harmonic distortion using FFT

While THD is calculated using FFT on Matlab Simulink for the output AC voltage when no optimization technique applied as the controller gains are selected by fine tuning, and equals 1.65%

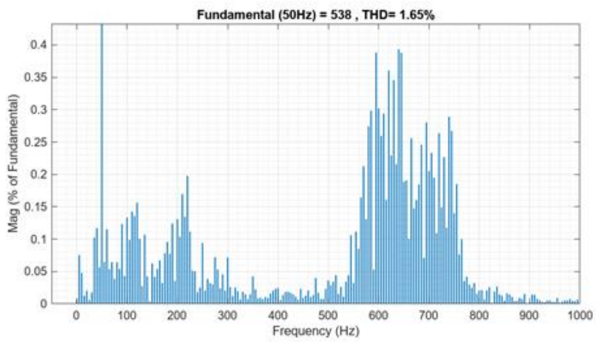

Fig 13. Total harmonic distortion using FFT

Induction motor is working at the rate conditions, figure 14 and figure 15 compares between rotor speed in both cases when JF is applied and without.

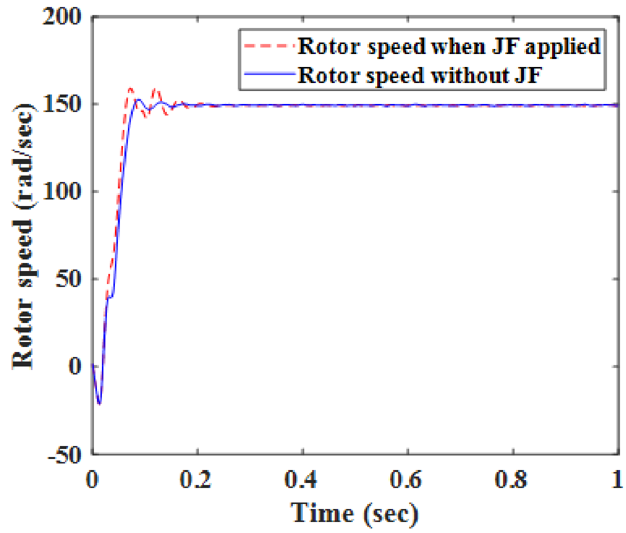

Fig 14. Rotor speed (rad/sec)

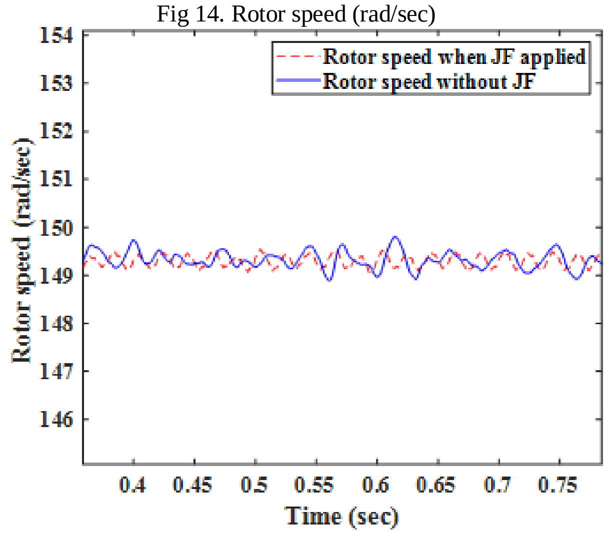

Fig 15. Rotor speed detailed (rad/sec)

Figure 15 shows that when JF optimization is applied on the system rotor speed ripples is much less than when JF isn't applied on the system.

7.CONCLUSION

Standalone PV water pumping system with battery storage is proposed in this paper. Proposed system consists of PV array, high gain DC-DC converter, bidirectional converter with battery, and 3-ph induction motor connected with the water pump. Jelly fish optimization tool has been applied on PI controllers to optimize controller gains for the system, THD for the output AC wave is 0.61%, and ripple factor for DC bus voltage is 0.2%, both are within acceptable limits. The proposed system is efficient and simple with no complex control technique. These advantage makes the proposed system suitable for Standalone PV-Based pumping applications.

8.References

[1] P. D. ,. P. K. B. L. M.-P. Jeba Singh Oliver, "Analysis of Grid-Interactive PV-Fed BLDC Pump Using," *Sustainability,* vol. 14, 2022.

[2] B. Kroposki, C. Pink, R. DeBlasio, H. Thomas, M. Simoes and P. Sen, "Benefits of power electronic interfaces for distributed energy systems," *Power Engineering Society General Meeting, IEEE`*, vol. 8, 2006.

[3] A. D. S. M. Mustapha Errouha, "Optimal Control of Induction Motor for Photovoltaic Water Pumping System," *Springer, Technology and Economics of Smart Grids and Sustainable Energy,* 2020.

[4] B. S. Saurabh Shukla, "Single-Stage PV-Grid Interactive Induction Motor Drive with Improved Flux Estimation Technique for Water Pumping with Reduced Sensors," *IEEE,* 2020.

[5] A. D. N. E. O. Mustapha Errouha, "High-Performance Standalone Photovoltaic Water Pumping System Using Induction Motor," *International Journal of Photo energy,* 2020.

[6] U. S. a. S. K. B. Singh, "Standalone photovoltaic water pumping system using induction motor drive with reduced sensors," *IEEE Transactions on Industry Applications,* vol. 54, p. 3645–3655, 2018.

[7] A. M. Z. M. M. E.-s. E. E. Aboul Zahab, "Design and control of a standalone PV water pumping system," *Journal of Electrical Systems and Information Technology,* vol. 4, p. 322–337, 2017.

[8] S. Kim, "Brushless direct current motors in Electric Motor Control," *Science Direct,* p. 389–416, 2017.

[9] A. B. O. M. A. A. S. Mohamed, "Optimized- fuzzy MPPT controller using GA for stand-alone photovoltaic water pumping system," in *40th Annual Conference of the IEEE Industrial Electronics Society*, Dallas, TX, USA, 2014.

[10] S. S. B. S. R. Rai, "Sensorless field oriented ISMCC for solar PV based induction motor drive for water pumping," *IEEE International Conference on Environment and Electrical Engineering,* 2019.

[11] J. A. B. S. M. Z. Salam, "The application of soft computing methods for MPPT of PV system: a technological and status review," *Applied Energy,* vol. 107, p. 135–148, 2013.

[12] J. A. A. A. M. A. H. M. A. Hannan, "Optimization techniques to enhance the performance of induction motor drives: a review," *Renewable and Sustainable Energy Reviews,* vol. 81, p. 1611–1626, 2018.

[13] A. C. A. E. H. e. a. S. Motahhir, "Optimal energy harvesting from a multistrings PV generator based on artificial bee colony algorithm," *IEEE Systems Journal,* pp. 1-8, 2020.

[14] W. Z. P. L. H. G. L. Shang, "Maximum power point tracking of PV system under partial shading conditions through flower pollination algorithm," *Protection and Control of Modern Power Systems,* vol. 3, 2018.

[15] X. A. Z. W. S. Salman, "Design of a P-&-O algorithm based MPPT charge controller for a stand-alone 200W PV system," *Protection and Control of Modern Power Systems,* vol. 3, 2018.

[16] N. Z. Y. Soladimeji Ibrahim, "Matlab/Simulink Model of Solar PV Array with Perturb and Observe MPPT for Maximising PV Array Efficiency," *IEEE Journal of Emerging and Selected Topics in Power Electronics,* vol. 6, 2018.

[17] D.-N. T. Jui-Sheng Chou, "A novel metaheuristic optimizer inspired by behavior of jellyfish in ocean," *ELSEVEIR, Applied Mathematics and Computation,* 2020.

[18] "DAB Pumps," DAB , 1982. [Online]. Available: https://www.dabpumps.com/en. [Accessed October 2022].

[19] A. G. A.-K. Dr Sameh S Ahemd, "Water-Pumping Using Powered Solar System - More Than an," *Journal of Energy and Natural Resources,* 2016.